

Modeling, Simulation and Analysis of 100Kw grid connected PV system using MATLAB/SIMULINK

Nisha Sharma

Asst. Prof. GJUS&T, Hisar, Haryana

Abstract: Increasing interest and investment in renewable energy give rise to rapid development of high penetration solar energy. Solar energy is most readily available source of energy. It is Non polluting and maintenance free. There are various models developed in MATLAB/SIMULINK to investigate different aspects of PV technology. In this paper a simulation model has been developed on MATLAB/SIMULINK. This model is developed on the basis of mathematical model of 100Kw grid connected photovoltaic (PV) generation system 'Vikram Solar Panel', installed at B.R.C.M College of Engineering & Technology, Bahal, Bhiwani, India. This module has 18 series and such 24 arrays parallel connected with 60 polycrystalline cells in each module. Taking the effect of irradiation and temperature into consideration, the output current, voltage and power characteristic of PV system are obtain. The results obtained are compared with the practical results. The simulated results are very close to the practical result.

Keywords: Maximum power point tracking, Photovoltaic (PV) system, Module, Grid connection.

I. INTRODUCTION

As a solution for the depletion of conventional fossil fuel energy sources and serious environmental problems, focus on the photovoltaic (PV) system has been increasing round the world. Since it is clean, pollution-free, and inexhaustible, researches on the PV power generation system have received much attention. Furthermore, for the continuing decrease in PV arrays cost and the increase in their efficiency, PV power generation system could be one of comparable candidates as energy sources for mankind in near future [1]. A photovoltaic system converts sunlight into electricity. The basic device of a photovoltaic system is the photovoltaic cell. Cells may be grouped to form panels or modules. Panels can be grouped to form large photovoltaic arrays. [2]. PV module represents the fundamental power conversion unit of a PV generator system. The output characteristics of PV module depends on the solar insolation, the cell temperature and output voltage of PV module. Since PV module has nonlinear characteristics, it is necessary to model it for the design and simulation of maximum power point tracking (MPPT) for PV system applications. The mathematical PV models used in computer simulation have been built for over the past four decades [3]-[4]. To make best use of the solar PV systems the output is maximized either by mechanically tracking the sun and orienting the panel in such a direction so as to receive the maximum solar irradiance or by electrically tracking the maximum power point under changing condition of insolation and temperature. The overall performance of solar cell varies with varying Irradiance and Temperature [5]-[6]. The PV application ranges from small installations of a few kW located in individual premises to large power plants generating several MW of power [7]-[8]. PV arrays are normally composed of large numbers of PV modules. These PV modules can have different current-voltage-

characteristics. The difference between module characteristics is called I-V mismatch. I-V mismatch can have permanent or temporary sources. Permanent sources cause - mismatch by changing one or more parameters in the PV module such as the value of parallel resistance and/or series resistance. Permanent sources include manufacturing tolerance, performance degradation, and module cracking. Power loss from manufacturing tolerance mismatch is below 1% for modern Si-modules [13]. These mismatch losses could increase due to aging to up to 2.4% [14]. A temporary source for I-V mismatch changes in the irradiance level received by PV modules. I-V mismatch caused by the changes in irradiance level is called partial shading of the PV array. Furthermore, partial shading sources could be divided into easy-to-predict and difficult-to-predict sources. Easy-to-predict sources include nearby PV arrays, buildings, and trees. Examples for difficult-to-predict sources are clouds soiling, and snow. Partial shading loss reduces annual energy yield by 5%-10% in Building Integrated Photovoltaic (BIPV) [15], [16] and by 3%-6% in PV farms [17]. Each module in the PV array should operate at its own maximum power point in order to maximize the power production of the PV array. This can be ensured by a single Maximum Power Point Tracker (MPPT) if there is no mismatch between the modules. In case of mismatch, there is no guarantee that all the modules are operating at their Maximum Power Points (MPPs). This can be avoided by having an MPPT for each PV module [18], [19]. Another solution is to use a multilevel inverter with independent voltage control for each PV module [20], [21]. In [22], it is proposed to connect all the modules in parallel to avoid these losses. AVARIETY of maximum power point tracking (MPPT) algorithms have been proposed including fractional open circuit voltage [23]-[24], fractional short circuit current

[25], [26], perturb and observe (P&O) [27]–[28], incremental conductance (INC) [29]–[30], and artificial-intelligence-based algorithms [17]–[21]. These algorithms vary in their complexity, efficiency, cost, and potential applications [27], [31], [32]. The main aim of this paper is to provide readers with the fundamental knowledge on how a model can be made on MATLAB/SIMULINK and how the simulated result can be compared with the actual results obtained from PV panel installed. The principle and operation of the PV cell and the fundamental characteristics of PV cell are discussed in para II. The simulation model developed using MATLAB/SIMULINK and the results obtained are presented and discussed in para III and the comparison of simulated result with that of practical result is discussed in para IV.

II. OPERATION AND CHARACTERISTICS OF PV OR SOLAR CELLS

During darkness, the solar cell is not an active device; it works as a diode, i.e a p-n junction. It produces neither a current nor a voltage. However, if it is connected to an external supply (large voltage), it generates a current I_D , called diode current or dark current [9]. The model contain a current source I_{ph} , one diode, a parallel resistance R_{sh} & a series resistance R_s , which represents the resistance inside each cell and in the connection between the cells. The net current is the difference between the photocurrent is the connection between the cells. The net current is given by the following equation:

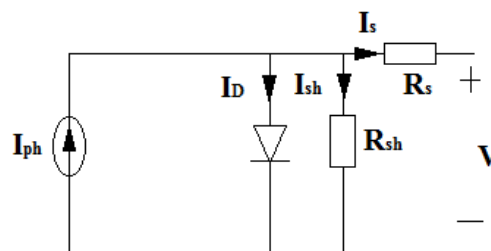


Fig.1 Circuit diagram of PV cell

$$I = I_{ph} - I_s \left(e^{\frac{q(V+IR_s)}{kTcA}} - 1 \right) - \frac{(V+IR_s)}{R_{sh}} \quad 1$$

Where A is idealizing factor, k is Boltzmann's gas constant, T_c the absolute temperature of the cell, q electronic charge & V is the voltage imposed across the cell. I_s is dark saturation current and it is strongly dependent on the temperature. PV system naturally exhibits a nonlinear I-V and P-V characteristics which

vary with the radiant intensity and cell temperature as shown in fig 2.

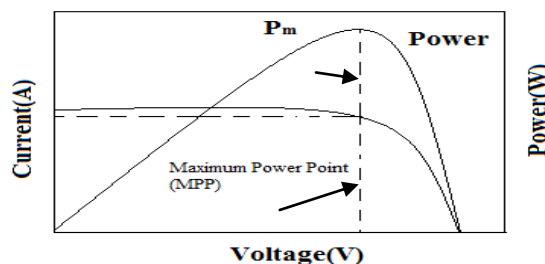


Fig.2 Characteristic curve of PV system.

III. MODELING AND SIMULATION OF PV CELL IN MATLAB/SIMULINK

The model is developed in MATLAB/SIMULINK based on the mathematical equation of PV cell. For developing the model, Vikram solar panel has been chosen. The Vikram Solar Panel, a 100 KW grid-connected photovoltaic (PV) generation systems have been installed at BRCM CET, Bahal.

In order to analyze the performance of grid connected PV system a model is developed in MATLAB and the curves obtained are compared with the actual values obtained. This module has 18 series and 24 parallel connected arrays with 60 polycrystalline cells in each module. This panel is installed in 2011 on the roofs of BRCM College

of Engineering and Technology, Bahal. The key specifications of the cell are shown in Table 1.

Target Tool used:

In this Dissertation work the tool used is SIMULINK models. To open that the path followed is

Library → SIMULINK → source

Library → SIMULINK → Math operation

Library → Simevent → Simevent Ports and Subsystem

This is the main model PV array System. In this system we have implemented the data of VIKRAM SOLAR ELDORA-235 installed at BRCM CET, Bahal. In this panel there are total 432 modules, in which 18 are connected in series and 24 such string in parallel with 60 cells per module.

Table1. Key specifications of the VIKRAM SOLAR PV Panel

Model	ELDORA 230
Cell type	Polycrystalline
Maximum Power[W]	(-0/+5w)(pump) 235w
Open circuit voltage V_{oc} [V]	36.65
Short Circuit Current I_{sc}	8.35
Current, Max power I_{mpp} [A]	8.08
Voltage , Max power V_{mpp} [V]	29.10
Temperature co-eff of V_{oc} (beta)	-0.32% / $^{\circ}C$
Temperature co-eff of I_{sc} (alpha)	0.04% / $^{\circ}C$
Temperature co-eff of power (gamma)	-0.45% / $^{\circ}C$
Normal operating cell temperature	45

A real solar cell can be characterized by the following fundamental parameters which are also sketched in model in Fig. 1.2

- a) Short circuit current $I_{sc}=I_{ph}$. It is the greatest value of the current generated by a cell. It is produced under short circuit condition $V=0$.
- b) Open circuit Voltage corresponding to the voltage drop across the diode (p-n junction), when it is traversed by the photocurrent I_{ph} (namely $I_D=I_{ph}$), namely when the

generated current is $I=0$. It reflects the voltage of the cell in the night and it can be mathematically expressed as:

$$V_{oc} = \frac{mkTc}{q} \ln \left(\frac{I_{ph}}{I_0} \right) = V_t \ln \left(\frac{I_{ph}}{I_0} \right) \quad 1$$

Where $V_t = \frac{mkTc}{q}$ is known as thermal voltage and T_c is the absolute cell temperature.

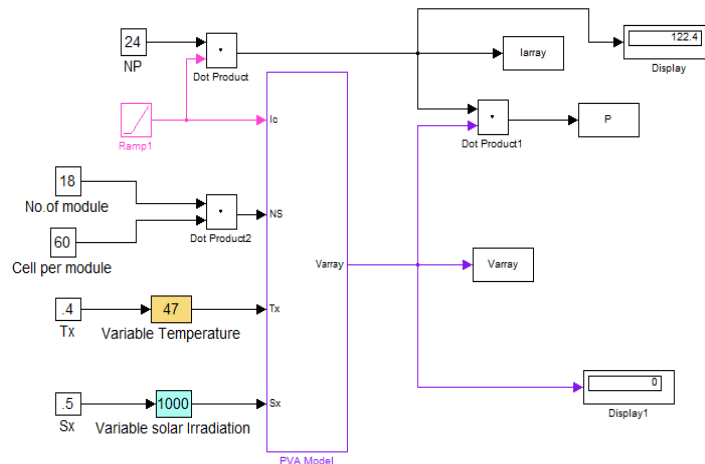


Fig 3. Main Model of PV array system

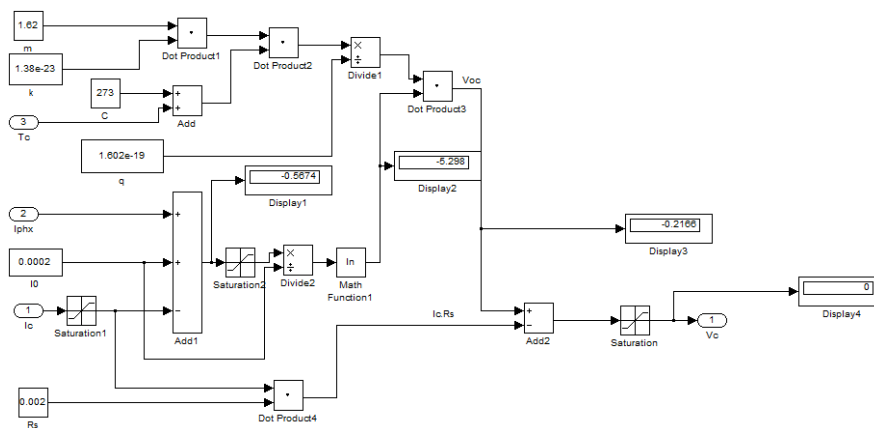


Fig 4. Model for V_c

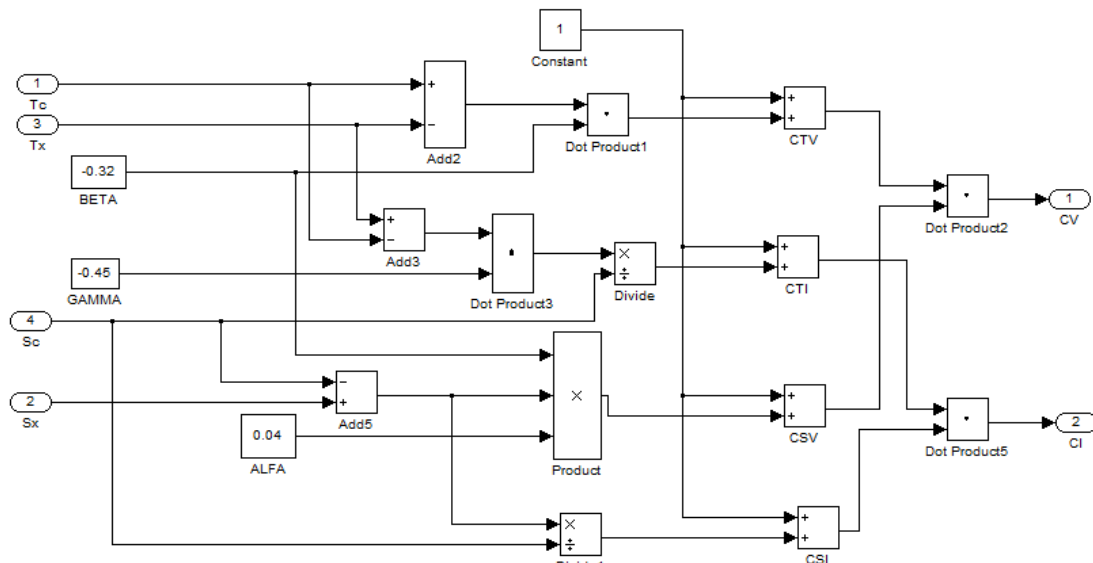


Fig 5 Model for CV and CI

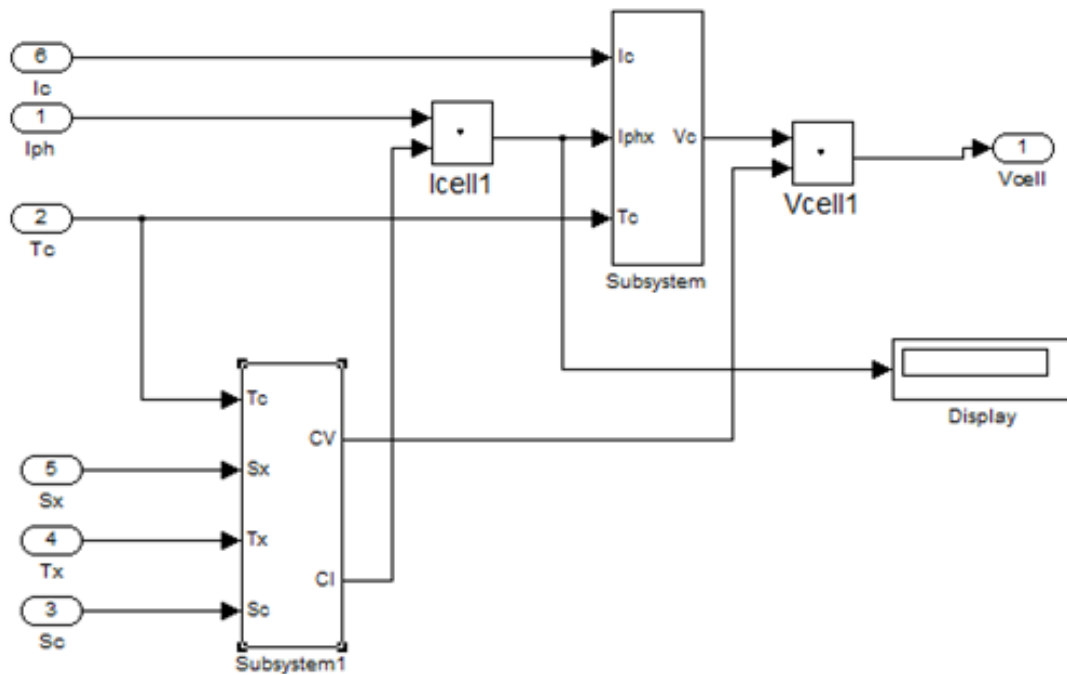


Fig 6 Model for V_{cell}

The light generated current of the photovoltaic cell depends linearly on the solar irradiation and is also influenced by the temperature according to the following equations [10]:

$$\begin{aligned}
 V_{CT} &= (T_c - T_x) \cdot \beta + 1 & 2 \\
 I_{CT} &= \frac{(T_c - T_x) \cdot \gamma}{S_c} + 1 & 3 \\
 V_{CS} &= \beta \cdot (S_c - S_x) \cdot \alpha + 1 & 4 \\
 I_{CS} &= \frac{S_c}{S_x} + 1 & 5 \\
 CV &= V_{CT} \cdot V_{CS} & 6 \\
 CI &= I_{CT} \cdot I_{CS} & 7 \\
 I_{ph} &= [I_{sc} + K_1(T_c - T_{ref})] \lambda & 8
 \end{aligned}$$

where I_{sc} is the cell's short-circuit current at a 25°C and 1kW/m², K_1 is the cell's short-circuit current temperature

coefficient, T_{ref} is the cell's reference temperature, and the solar insolation in kW/m². [11]-[12].

$$V_{cell} = V_c \cdot CV \tag{9}$$

Here V_c is that constant voltage of the cell which is define during its fabrication and CV is that voltage which is obtained due to effect of temperature and irradiation. The output of the models can be obtained on different temperature and different irradiation value. The outputs of simulated output are shown in the tables and graphs. Fig 5.1 shows that when temperature 46.4°C and irradiation 1000 watt/m², value of I_{max} is 110 A, V_{max} is 903V and P_{max} is 100 kW .

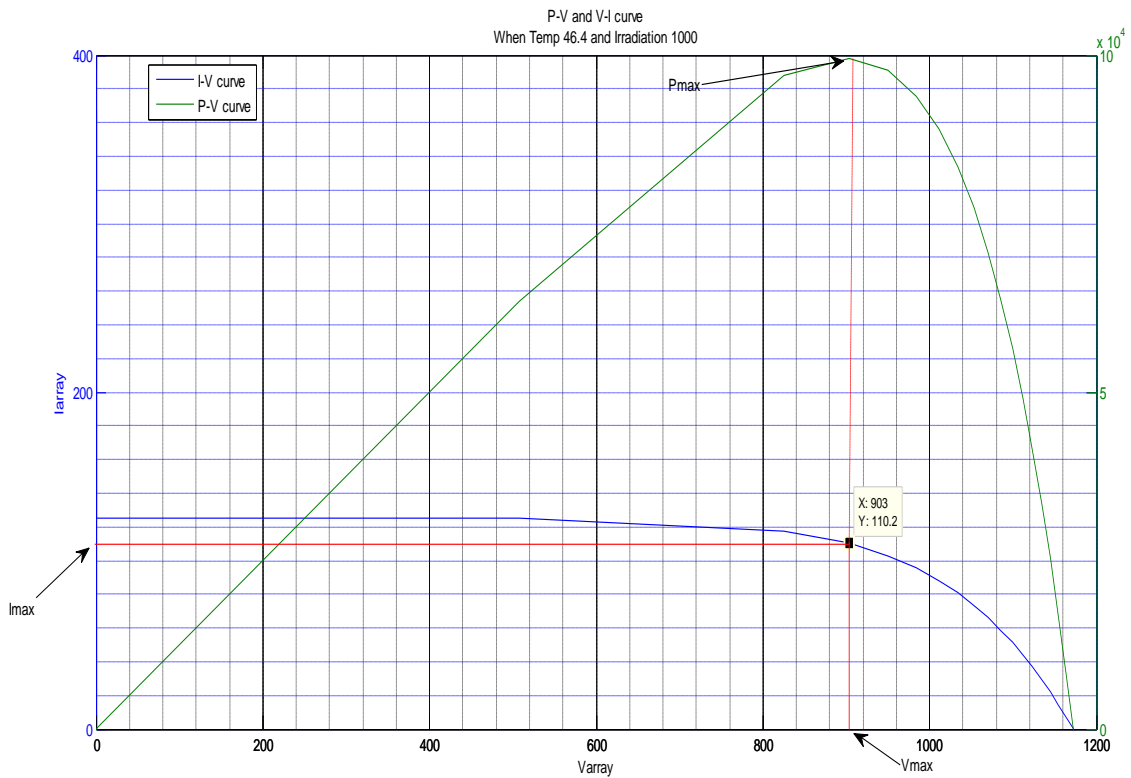


Fig. 5.1 Variation of P, V & I at Temp 46.4 °C and Irradiation 1000 watt/m²

Fig 5.2 shows that when temperature 46.4°C and irradiation 600 watt/m², value of I_{max} is 66.1 A, V_{max} is 1306V and P_{max} is 86.3 kW .

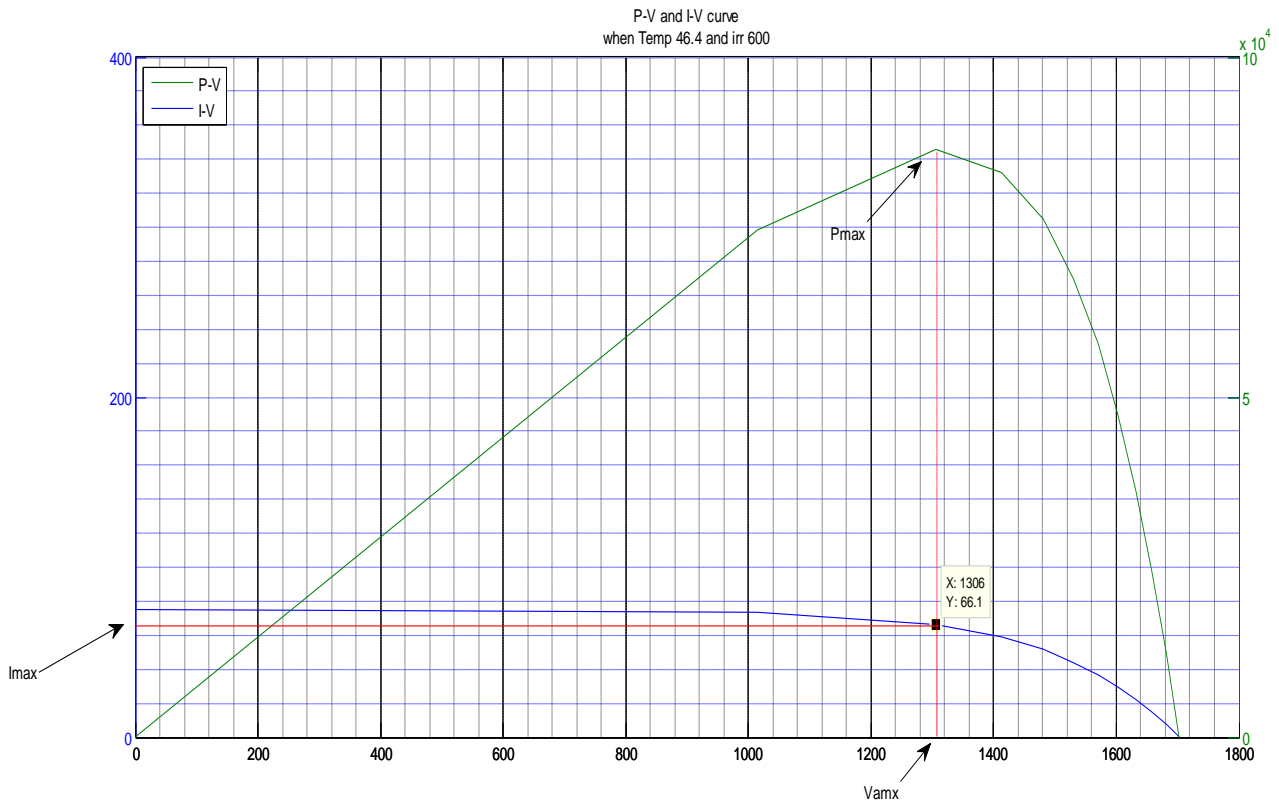


Fig. 5.2 Variation of P, V & I at temp 46.4 °C and Irradiation 600 watt/m²

Fig 5.3 shows that when temperature 45 °C and irradiation 800 watt/m², value of I_{max} is 88.1 A, V_{max} is 745.3V and P_{max} is 65.6 kW .

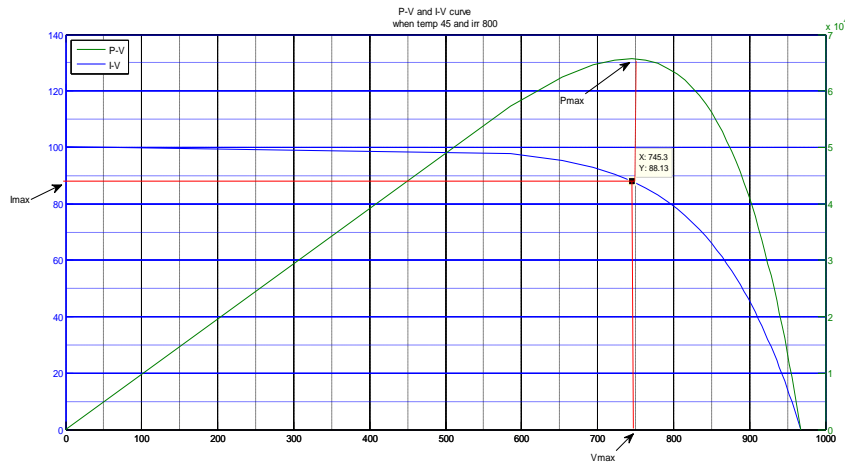


Fig. 5.3 Variation of P, V & I at Temp 45 °C and Irradiation 800 watt/m²

Fig 5.4 shows that when temperature 45 °C and irradiation 400 watt/m², value of I_{max} is 44 A, V_{max} is 973V and P_{max} is 42.8 kW .

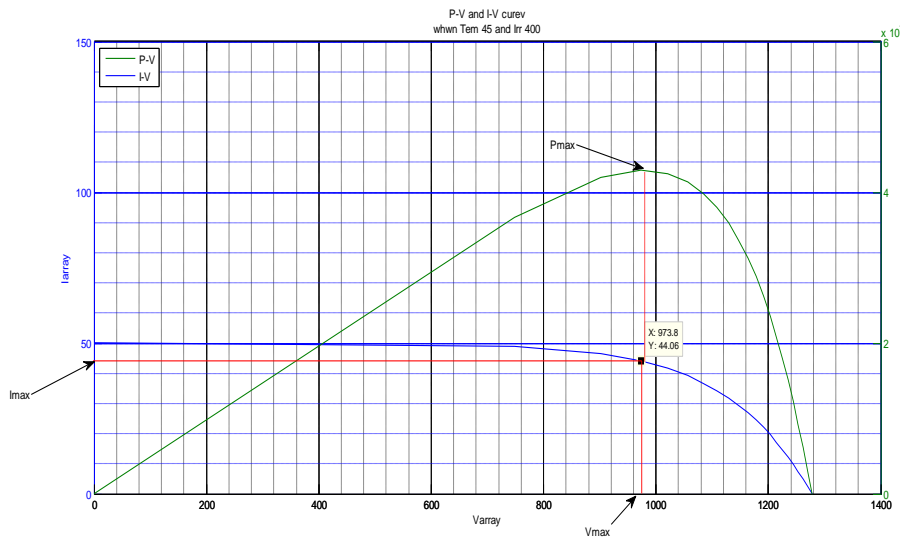


Fig. 5.4 Variation of P, V & I at Temp 45 °C and Irradiation 400 watt/m²

Fig 5.5 shows that when temperature 45 °C and irradiation 200 watt/m², value of I_{max} is 22.1 A, V_{max} is 1015V and P_{max} is 22.3 kW .

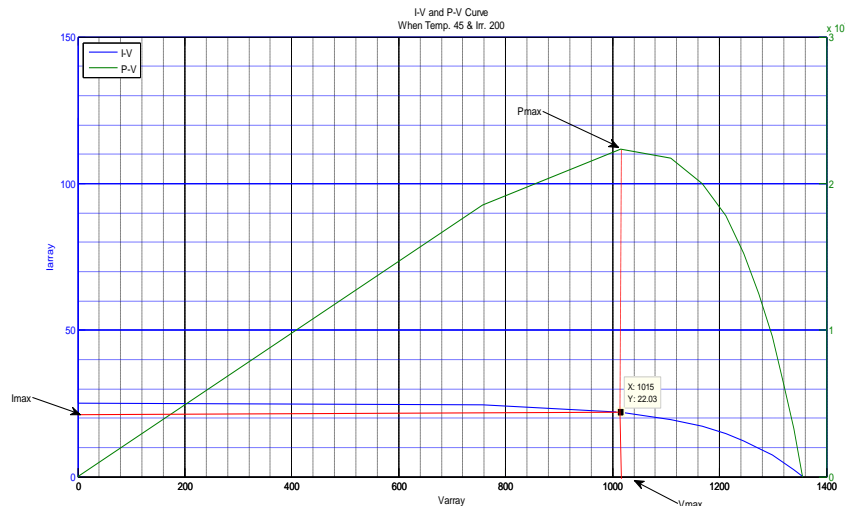


Fig. 5.5 Variation of P, V & I at Temp 45 °C and Irradiation 200 watt/m²

Fig 5.6 shows that when temperature 44°C and irradiation 1000 watt/m^2 , value of I_{max} is 110.2 A , V_{max} is 388.8V and P_{max} is 42.8 kW .

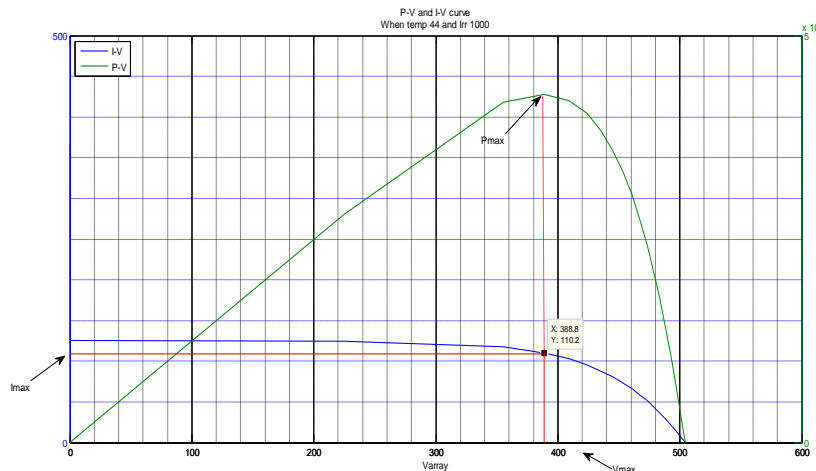


Fig. 5.6 Variation of P, V & I at Temp 44°C and Irradiation 1000 watt/m^2

Fig 5.7 shows that when temperature 44°C and irradiation 800 watt/m^2 , value of I_{max} is 88.1 A , V_{max} is 480.4V and P_{max} is 42.3 kW .

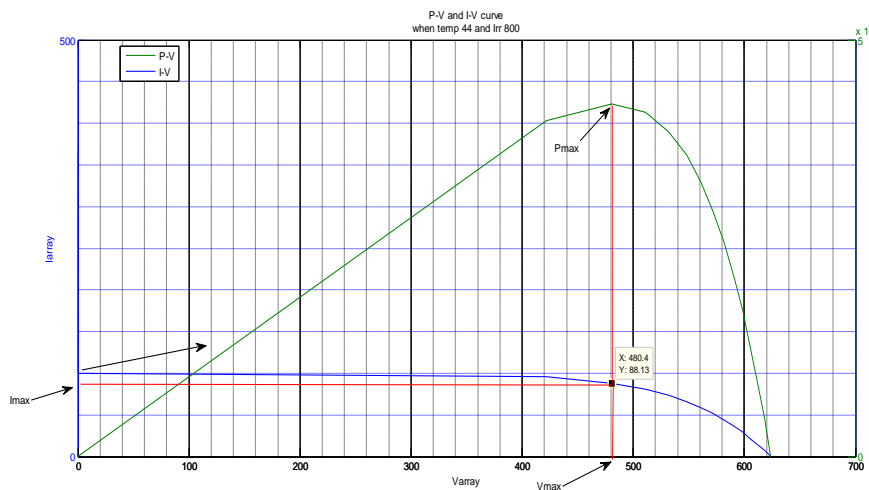


Fig.5.7 Variation of P, V & I at Temp 44°C and Irradiation 800 watt/m^2

Fig 5.8 shows that when temperature 44°C and irradiation 600 watt/m^2 , value of I_{max} is 66.1 A , V_{max} is 562.5V and P_{max} is 37.1 kW .

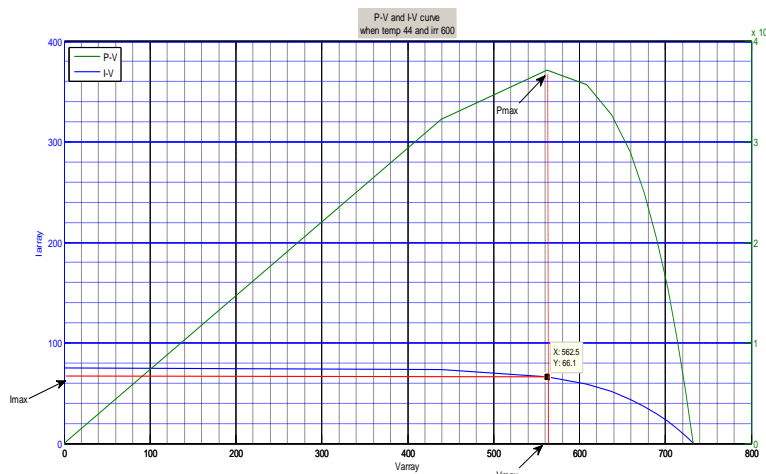


Fig. 5.8 Variation of P, V & I at Temp 44°C and Irradiation 600 watt/m^2

Fig 5.9 shows that when temperature 44°C and irradiation 400 watt/m^2 , value of I_{max} is 44.6 A , V_{max} is 627.7V and P_{max} is 27.9 kW .

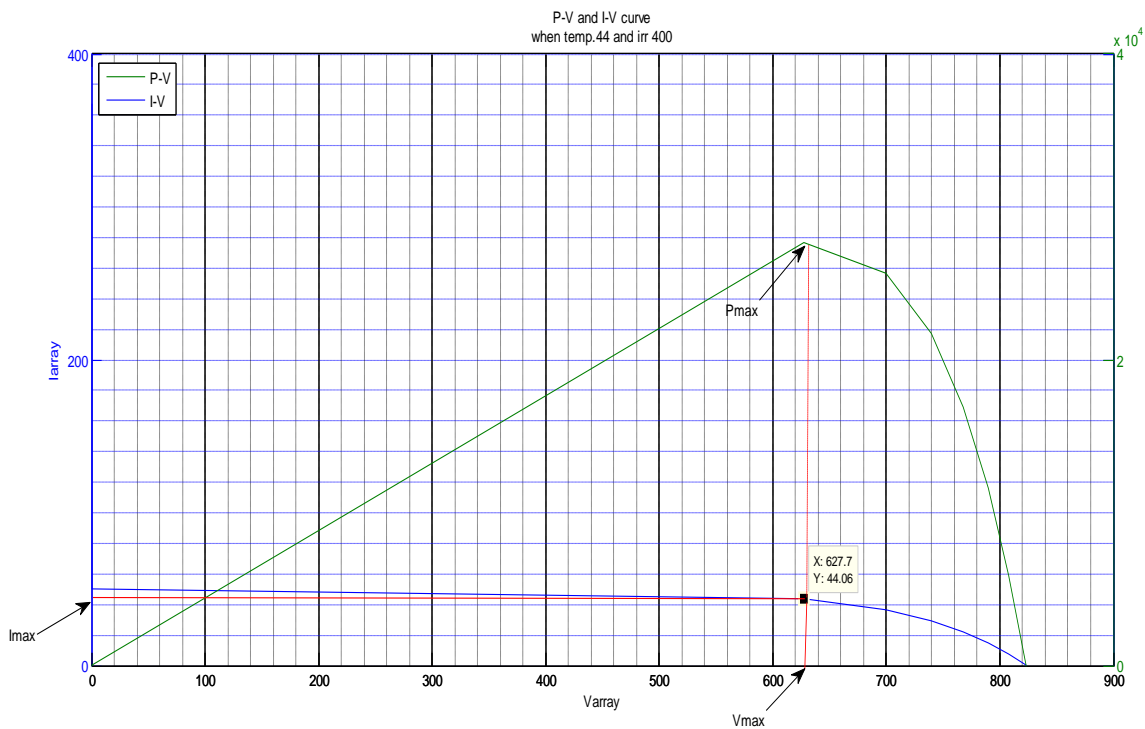


Fig. 5.9 Variation of P, V & I at Temp 44°C and Irradiation 400 watt/m^2

Fig 5.10 shows that when temperature 44°C and irradiation 200 watt/m^2 , value of I_{max} is 22.03 A , V_{max} is 645.2V and P_{max} is 14.4 kW .

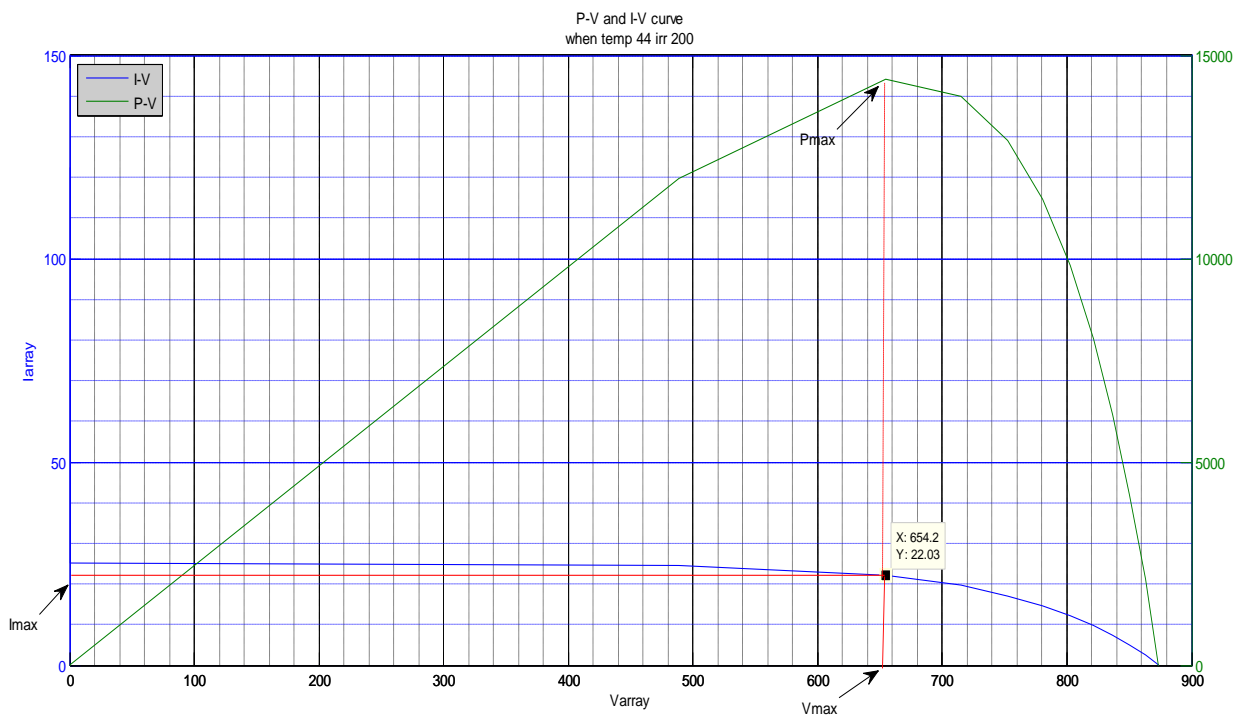


Fig. 5.10 Variation of P, V & I at Temp 44°C and Irradiation 200 watt/m^2

Fig 5.11 shows that when temperature 43°C and irradiation 800 watt/m^2 , value of I_{max} is 88.1 A , V_{max} is 215.4V and P_{max} is 18.9 kW .

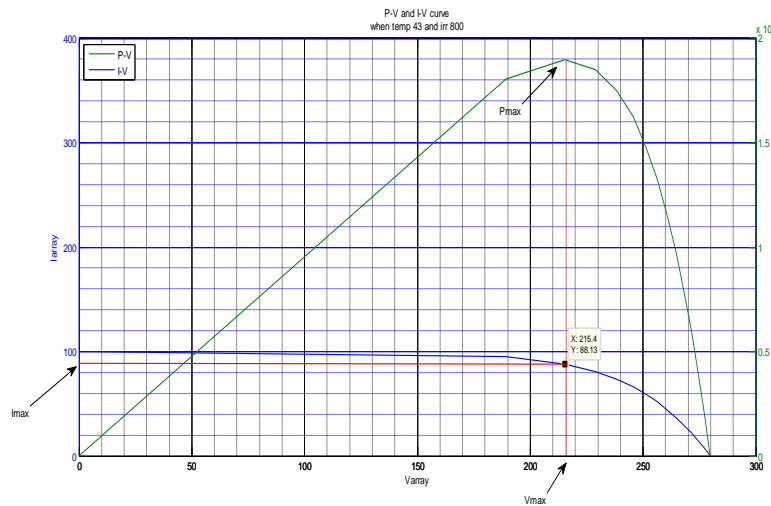


Fig. 5.12 Variation of P, V & I at Temp 43 °C and Irradiation 800 watt/m²

Fig 5.13 shows that when temperature 43 °C and irradiation 600 watt/m², value of I_{max} is 66.1 A, V_{max} is 252V and P_{max} is 16.6 kW.

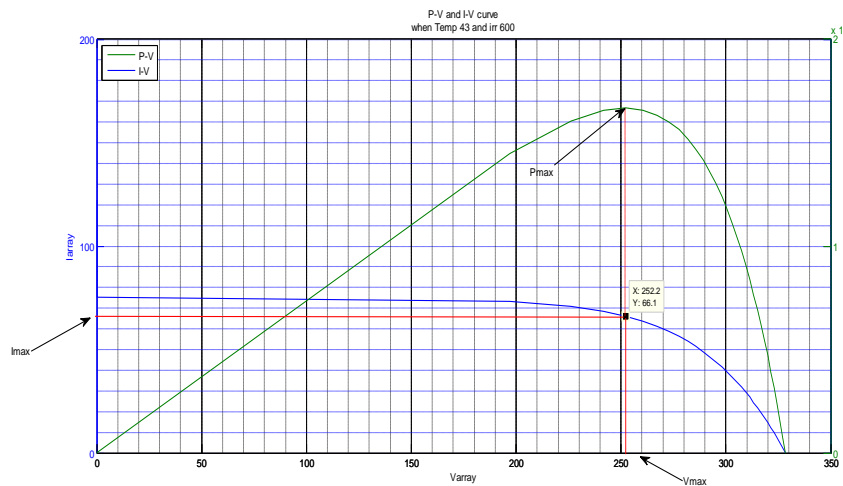


Fig. 5.13 Variation of P, V & I at Temp 43 °C and Irradiation 600 watt/m²

Fig 5.14 shows that when temperature 43 °C and irradiation 400 watt/m², value of I_{max} is 44.06 A, V_{max} is 281.4V and P_{max} is 12.3 kW .

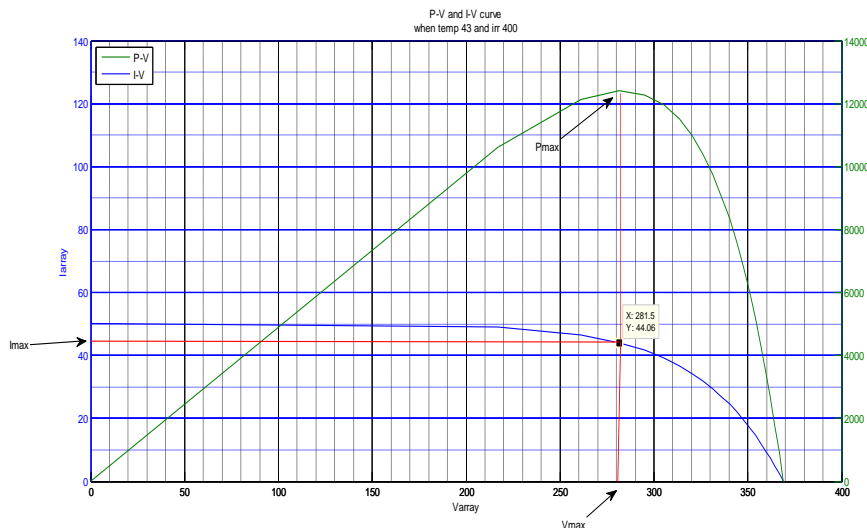


Fig. 5.14 Variation of P, V & I at Temp 43 °C and Irradiation 400 watt/ m²

Fig 5.15 shows that when temperature 43°C and irradiation 200 watt/m^2 , value of I_{max} is 22.03 A , V_{max} is 293.4V and P_{max} is 6.6 kW .

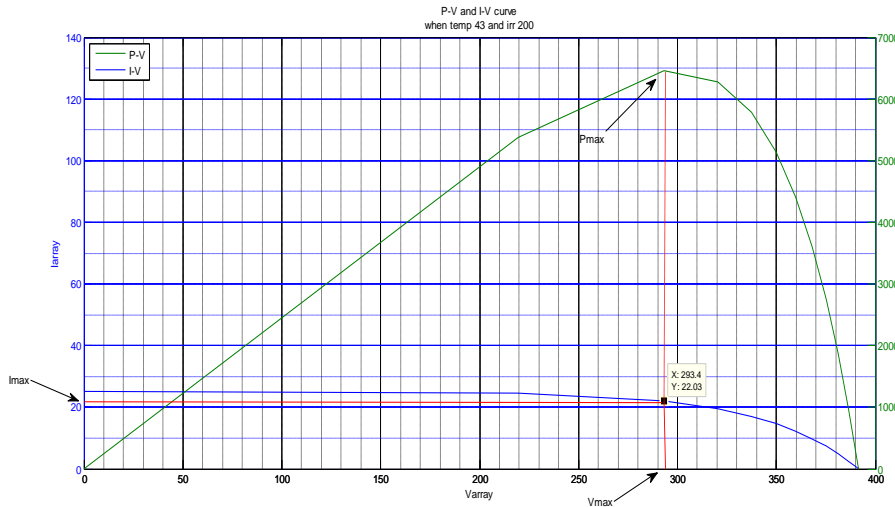


Fig. 5.15 Variation of P, V & I at Temp 43°C and Irradiation 200 watt/m^2

The graph shows the variation of Power, Current and simulated results, following data are predicted as voltage according to temperature and irradiation. The open circuit Voltage increase logarithmically with the ambient different voltage current, and power dependent on irradiation, while the short circuit current is a linear irradiation and constant temp 46.4°C function of the ambient irradiation. From the above

Table 5.1 Maximum Power when Temperature 46.4°C

S. NO	SET: 1	V_{max} (Model in Matlab)	I_{max} (Model in Matlab)	P_{max} (Model in Matlab)
1.	Irradiance: 200 watt/m^2	1519	22.1	33.5
2.	Irradiance: 400 watt/m^2	1458	44	64.1
3.	Irradiance: 600 watt/m^2	1306	66.1	86.3
4.	Irradiance: 800 watt/m^2	1116	88	98.2
5.	Irradiation 1000 watt/m^2	903	110	100

Now when Temperature 45°C

Table 5.2 Maximum Power when Temperature 45°C

S. NO	SET: 1	V_{max} (Model in Matlab)	I_{max} (Model in Matlab)	P_{max} (Model in Matlab)
1.	Irradiance: 200 watt/m^2	1015	22.1	22.3
2.	Irradiance: 400 watt/m^2	973	44	42.8
3.	Irradiance: 600 watt/m^2	872.6	66.1	57.6
4.	Irradiance: 800 watt/m^2	745.3	88.1	65.6
5.	Irradiation 1000 watt/m^2	551.3	117.5	64.7

Now when Temperature 44°C

Table 5.3 Maximum Power when Temperature 44°C

S. NO	SET: 1	V_{max} (Model in Matlab)	I_{max} (Model in Matlab)	P_{max} (Model in Matlab)
1.	Irradiance: 200 watt/m^2	654.2	22.03	14.4
2.	Irradiance: 400 watt/m^2	627.7	44.6	27.9
3.	Irradiance: 600 watt/m^2	562.5	66.1	37.1
4.	Irradiance: 800 watt/m^2	480.4	88.1	42.3
5.	Irradiation 1000 watt/m^2	388.8	110.2	42.8

Now, when Temperature 43⁰C

Table 5.4 Maximum Power when Temperature 43⁰C

S. NO	SET: 1	V _{max} (Model in Matlab)	I _{max} (Model in Matlab)	P _{max} (Model in Matlab)
1.	Irradiance:200 watt/m ²	293.4	22.03	6.6
2.	Irradiance:400 watt/m ²	281.4	44.06	12.3
3.	Irradiance: 600 watt/m ²	252	66.1	16.6
4.	Irradiance: 800 watt/m ²	215.4	88.1	18.9
5.	Irradiation 1000 watt/m ²	174.3	110.2	19.2

IV. CONCLUSION

The performance of PV system is strongly dependant on meteorological conditions such as shading, irradiance, PV array surface temperature, etc. Therefore, the performance

of PV arrays was analyzed using the measured performance results of PV systems for monitoring period and investigated by reviewing several problems such as performance deterioration and losses. Data obtained from VIKRAM SOALR PANEL

Table 5.5 Comparison of data of VIKRAM SOLAR PANEL and Simulated result in MATLA

S. No.	SET: 1	Temp (°C)	V _{max} (V) (Vikram solar Panel)	V _{max} (V) (Model in Matlab)	I _{max} (A) (Vikram solar Panel)	I _{max} (A) (Model in Matlab)	P _{max} (kW) (Vikram solar Panel)	P _{max} (kW) (Model in Matlab)
1.	Irradiance: 200 watt/m ²	40	78	156	27	22	2.1	3.4
2.	Irradiance: 400 watt/m ²	43	167	211.4	50	44.06	8.3	9.3
3.	Irradiance: 600 watt/m ²	45	767	872.6	70	66.1	53.2	57.6
4.	Irradiance: 800 watt/m ²	46	903	1116	88	88	79.4	98.2
5.	Irradiation: 1000 watt/m ²	44	402	388.8	131	110.2	52.2	42.8

A photovoltaic VIKRAM SOLAR PANEL has been analyzed, installed at the BRCM College of Engineering and Technology. It has been found that, on average, the real power of the modules is 10% lower than the nominal power given by the manufacturer. The mean daily energy generated by our installation has been 60 kWh. They are due, basically, to the strong dependence of the inverter threshold losses on daily irradiation. Thus, on days with low irradiation, the inverter is not able to make connection with the grid. For analysis of the panel one Model is made on MATLAB/SIMULINK. Then the data from the manufacture sheet is applied on the model, the output are then compared with realistic value of the VIKRAM SOLAR PANEL. So from the Tables obtained we can see that for a good efficiency Temperature must be 46.4⁰C and Irradiation must be 1000 watt/m². But when data is collected from the VIKRAM SOLAR we obtain that it reaches to maximum efficiency upto 79% even in most hot day.

REFERENCE

[1] Jung Hun So, Young Seok Jung, Gwon Jong Yu, Ju Yeop Choi, Jae Ho Choi, Performance results and analysis of 3 kW grid-connected PV systems,elsevir Renewable Energy 32 (2007) pp. 1858–1872.
[2] Marcelo Gradella Villalva, Jonas Rafael Gazoli, Ernesto Ruppert Filho, MODELING AND CIRCUIT-BASED SIMULATION OF PHOTOVOLTAIC ARRAYS, 10th Brazilian Power Electronics Conference (COBEP), 2009

[3] S. W. Angrist, , Direct Energy Conversion, Allyn and Bacon, Inc., 4th edition, 1982, pp. 177-227.
[4] J. C. H. Phang, D. S. H. Chan, and J. R. Philips, “Accurate analytical method for the extraction of solar cell model parameters,” Electronics Letters, vol. 20, no. 10, 1984, pp.406-408.
[5] Pradhan Arjyadhara1, Ali S.M2, Jena Chitralekha3, Analysis of Solar PV cell Performance with Changing Irradiance and Temperature., International Journal Of Engineering And Computer Science ISSN:2319-7242 Volume 2 Issue 1 Jan 2013 Page No. 214-220.
[6] ‘Lee, Kui-Jun et al ; An Adaptive Maximum Power Point Tracking Scheme Based on a Variable Scaling Factor for Photovoltaic Systems’, The Korean Institute of Power Electronics, May 2012, Volume 17, pp.423-430.
[7] G.Petrona and C.A.Ramos - Pajab, Modeling of photovoltaic fields in mismatched conditions for energy yield evaluations, ”Elect. Power Syst. Res.,vol.81,no.4, pp.1003-1013,Apr.2011.
[8] B.InduRani, Member, IEEE, G.Saravananlango, and Chilakapati Nagamani, Member, IEEE, Enhanced Power Generation From PV Array Under Partial Shading Conditions by Shade Dispersion Using Su Do Ku Configuration. IEEE TRANSACTIONS ON SUSTAINABLE ENERGY November14,2012 pp. 1-7.
[9] S. Sheik Mohammed, ‘Modeling and Simulation of Photovoltaic module using MATLAB/Simulink’, International Journal of Chemical and Environmental Engineering Volume 2, No.5, October 2011. 350-355
[10] Huan-Liang Tsai, Ci-Siang Tu, and Yi-Jie Su, Member, IAENG ‘Development of Generalized Photovoltaic Model Using MATLAB/SIMULINK’, Proceedings of the World Congress on Engineering and Computer Science 2008 WCECS 2008, October 22 - 24, 2008, San Francisco, USA.
[11] Anca D. Hansen, ‘Models for a Stand-Alone PV System’, Riso-R-1219(EN)SE C-R-12, Risco National Laboratory, Roskilde , December 2000 pp. 1-78.
[12] M. Sidrach-de-Cardona, Ll. Mora Lo´pez, Performance analysis of a grid-connected photovoltaic system, pergamon, Energy 24 (1999) 93–102.

- [13] F. Spertino and J. S. Akilimali, "Are manufacturing I-V mismatch and reverse currents key factors in large photovoltaic arrays?," *IEEE Trans. Ind. Electron.*, vol. 56, no. 11, pp. 4520–4531, Nov. 2009.
- [14] N. D. Kaushika and A. K. Rai, "An investigation of mismatch losses in solar photovoltaic cell networks," *Energy*, vol. 32, no. 5, pp. 755–759, May 2007. SHAMS EL-DEIN et al.: OTCT INTERCONNECTION FOR REDUCING MISMATCH LOSSES IN PV ARRAYS 107
- [15] M. Drif, P. J. Perez, J. Aguilera, and J. D. Aguilar, "A new estimation method of irradiance on a partially shaded PV generator in gridconnected photovoltaic system," *Renew. Energy*, vol. 33, no. 9, pp. 2048–2056, Feb. 2008.
- [16] The German Energy Society, *Planning and Installing Photovoltaic Systems: A Guide for Installers, Architects, and Engineers* Earth scan, London, Sterling, VA, 2008, pp. 152–157.
- [17] M. García, J. A. Vera, L. Marroyo, E. Lorenzo, and M. Pérez, "Solartracking PV plants in Navarra: A 10 MW assessment," *Progress in Photovoltaics: Res. Applicat.*, vol. 17, no. 5, pp. 337–346, Aug. 2009.
- [18] N. Femia, G. Lisi, G. Petrone, G. Spagnuolo, and M. Vitelli, "Distributed maximum power point tracking of photovoltaic arrays: Novel approach and system analysis," *IEEE Trans. Ind. Electron.*, vol. 55, no. 7, pp. 2610–2621, Jul. 2008.
- [19] E. Roman, R. Alonso, P. Ibanez, S. Elorduizapatarietxe, and D. Goitia, "Intelligent PV module for grid-connected PV systems," *IEEE Trans. Ind. Electron.*, vol. 53, no. 4, pp. 1066–1073, Jun. 2006.
- [20] S. Busquets-Monge, J. Rocabert, P. Rodriguez, S. Alepuz, and J. Bordonau, "Multilevel diode-clamped converter for photovoltaic generators with independent voltage control of each solar array," *IEEE Trans. Ind. Electron.*, vol. 55, no. 7, pp. 2713–2723, Jul. 2008.
- [21] A. I. Bratcu, I. Munteanu, S. Bacha, D. Picault, and B. Raison, "Cascaded DC-DC converter photovoltaic systems: Power optimization issues," *IEEE Trans. Ind. Electron.*, vol. 58, no. 2, pp. 403–411, Feb. 2011.
- [22] L. Gao, R. A. Dougal, S. Liu, and A. P. Iotova, "Parallel-connected solar PV system to address partial and rapidly fluctuating shadow conditions," *IEEE Trans. Ind. Electron.*, vol. 56, no. 5, pp. 1548–1556, May 2009.
- [23] J. H. R. Enslin, M. S. Wolf, D. B. Snyman, and W. Swiegers, "Integrated photovoltaic maximum power point tracking converter," *IEEE Trans. Ind. Electron.*, vol. 44, no. 6, pp. 769–773, Dec. 1997.
- [24] M. A. Elgendy, B. Zahawi, and D. J. Atkinson, "Comparison of directly connected and constant voltage controlled photovoltaic pumping systems," *IEEE Trans. Sustain. Energy*, vol. 1, no. 3, pp. 184–192, Oct. 2010.
- [25] M. F. Mimouni, M. N. Mansouri, B. Benghanem, and M. Annabi, "Vectorial command of an asynchronous motor fed by a photovoltaic generator," *Renew. Energy*, vol. 29, pp. 433–442, 2004.
- [26] S. Yuvarajan, D. Yu, and S. Xu, "A novel power converter for photovoltaic applications," *J. Power Sources*, vol. 135, pp. 327–331, 2004.
- [27] V. Salas, E. Olias, A. Barrado, and A. Lazaro, "Review of the maximum power point tracking algorithms for stand-alone photovoltaic systems," *Solar Energy Mater. Solar Cells*, vol. 90, pp. 1555–1578, 2006.
- [28] A. Pandey, N. Dasgupta, and A. K. Mukerjee, "High-performance algorithms for drift avoidance and fast tracking in solar MPPT system," *IEEE Trans. Energy Convers.*, vol. 23, no. 2, pp. 681–689, Jun. 2008.
- [29] K. H. Hussein, I. Muta, T. Hoshino, and M. Osakada, "Maximum photovoltaic power tracking: an algorithm for rapidly changing atmospheric conditions," *IEE Proc., Generation, Transmission and Distribution*, vol. 142, pp. 59–64, 1995.
- [30] A. Safari and S. Mekhilef, "Simulation and hardware implementation of incremental conductance MPPT with direct control method using cuk converter," *IEEE Trans. Ind. Electron.*, vol. 58, no. 4, pp. 1154–1161, Apr. 2011
- [31] D. P. Hohm and M. E. Ropp, "Comparative study of maximum power point tracking algorithms," *Progress in Photovoltaics: Research and Applications*, vol. 11, pp. 47–62, 2003.
- [32] T. Easram and P. L. Chapman, "Comparison of photovoltaic array maximum power point tracking techniques," *IEEE Trans. Energy Convers.*, vol. 22, no. 2, pp. 439–449, Jun. 2007.